PERGAMON

International Journal of Mechanical Sciences 44 (2002) 79–101

International Journal of MECHANICAL SCIENCES

www.elsevier.com/locate/ijmecsci

Measurement of springback

W.D. Carden[a], L.M. Geng[a], D.K. Matlock[b], R.H. Wagoner[a,*]

[a] *Department of Materials Science and Engineering, The Ohio State University, 177 Watts Hall, 2041 College Road, Columbus, OH 43210-1179, USA*

[b] *Colorado School of Mines, Department of Metallurgical Engineering, Golden, CO 80401, USA*

Received 16 May 2000; received in revised form 2 July 2001

Abstract

Springback, the elastically-driven change of shape of a part after forming, has been measured under carefully-controlled laboratory conditions corresponding to those found in press-forming operations. Constitutive equations emphasizing low-strain behavior were generated for three automotive body alloys: drawing-quality silicon-killed steel; high-strength low-alloy steel; and 6022-T4 aluminum. Strip draw-bend tests were then conducted using a range of die radii ($3 < R/t < 17$), friction coefficients ($0 < \mu < 0.20$), and controlled tensile forces ($0.5 < F_b/F_y < 1.5$). Springback angles and curvatures were measured for bend and bend–unbend areas of the specimen, the latter corresponding to the "sidewall curl" region, which dominates the geometric change and the dependence on process variables. Friction coefficient and R/t (die-radius-to-sheet-thickness) greater than 5 have modest but measurable effects over the ranges tested. As expected, strip tension dominates the springback sensitivity, with higher forces reducing springback. For 6022-T4, springback is dramatically reduced as the tensile stress approaches the yield stress, corresponding to the appearance of a persistent anticlastic curvature. The presence of this curvature, orthogonal to the principal curvature, violates the simple two-dimensional models of springback reported in the literature. The measured springback angles and curvatures are reported both in graphical summary and tabular form for use in assessing analytical models of springback. © 2002 Elsevier Science Ltd. All rights reserved.

Keywords: Springback; Sheet metal forming; Anticlastic curvature; DQSK steel; 6022-T4 aluminum; HSLA steel; Draw–bend tests; Plastic anisotropy

1. Introduction

Springback, the elastically-driven change in shape of a part upon unloading after forming, is a growing concern as manufacturers increasingly rely on materials with higher strength-to-modulus

* Corresponding author. Tel.: +1-614-292-2079; fax: +1-614-292-6530.
E-mail address: wagoner.2@osu.edu (R.H. Wagoner).

0020-7403/02/$ - see front matter © 2002 Elsevier Science Ltd. All rights reserved.
PII: S0020-7403(01)00082-0

Nomenclature

h	arc height at the center of the strip
F_b	actual back force
F_y	yield force
$\overline{F_b}$	normalized back force
F_f	actual front force
R	tool radius
R_a	anticlastic radius of curvature on the curl region
R', θ_1	radius and corresponding angle for the region of sheet strip that has undergone only bending
r', θ_2	radius and corresponding angle for the region of sheet strip that has undergone both bending and straightening
t	sheet thickness
w	arc width of the sheet strip cross section
θ	overall springback angle of sheet strip
κ_a	anticlastic curvature on the curl region
μ	friction coefficient

ratios than the traditional low-strength steel. High-strength low-alloy steel (HSLA) and 6022-T4 aluminum alloy are frequently considered as direct replacements for drawing-quality silicon-killed steel (DQSK), the current mainstay for automotive body panels.

Corrections for springback are essential during die design in order to obtain specified final shapes. Correction curves based on empirical information or simple theories for small-springback in pure bending cases have been available for many decades [1–3] based on the basic assumptions of engineering beam bending. Many analytical solutions have been derived, and with reviews have appeared for the early work [4,5], and more recently [6,7].

While the literature dealing with analysis of springback of metal sheets is extensive, carefully-controlled experiments of springback under realistic forming conditions (i.e. involving bending and unbending simultaneous with imposed tension and sliding over the tooling) are less common. Many experiments have been carried out under pure-bending (i.e. with minimal tension) conditions of various kinds: cylindrical tooling [8–10], U-bending/channel bending [11–13], V-bending [12–14], and flanging [15]. Such experiments show springback increasing with R/t (tool radius/sheet thickness), but such results have little application to situations where significant sheet tension is present, because sheet tension dominates other process variables in determining springback.

Stretch-bend tests [13,16,17] allow careful control of sheet tension during bending, but do not typically exhibit bending and unbending, nor large sliding over the tooling common in press forming operations. These tests do show, however, the pervasive effect of sheet tension on springback, especially for sheet tensile stresses in the range of the material yield stress.

Actual forming operations, such as a two-dimensional idealization of draw/stretch bending of a flanged channel (also called a top-hat section) are used to assess practical springback. This geometry

is the most studied of springback cases [18–24] (including benchmark testing and simulations [25]) because of its practical importance, and because of the obvious, measurable presence of sidewall curl. However, in such operations, the sheet tension is determined only indirectly, either from the blank holder force, or from a drawbead simulation [26–29], both of which depend on the coefficient of friction, which is usually known only approximately. Because of the dominant role of sheet tension in springback, lack of control or direct measurement of this quantity is a serious drawback for scientific use of such experiments in verifying simulation techniques. Such operations have common features, including reduced springback and curl for increased blank holder forces (especially when sheet tension approaches the yield stress). Curl has been shown to disappear as R/t approaches 2 for a variety of steels [18,22,24]. For smaller R/t, the curl may reverse direction.

The exceptional work is by Liu [30] for flanged channels, and Kuwabara et al. [31] for draw-bending. Liu devised a special channel flanging experiment in which the restraining force was applied directly by a controlled hydraulic cylinder. In this way, sidewall curl and springback could be assessed in terms of known restraining forces for several materials. Kuwabara et al. used a draw–bend apparatus that appears similar to the one in the current work, although dimensions and specifications were not provided [31]. Reported springback angles decreased with increasing R/t and the usual dependence on sheet tension was observed. The current draw/bend test [32–34], conceived for friction testing, is similar in concept to Liu's experiment, with four significant differences of the current device:

(1) much longer drawn distances are attainable, with correspondingly increased precision of shape measurement,
(2) there is no bend at the bottom of the channel to complicate interpretation,
(3) there is only a single tool, thus avoiding changing clearances and geometries during the punch stroke, and
(4) the material hardening curves were measured and fit in some detail.

The sensitivity of springback to a Bauschinger effect, particularly for bend/unbend operations (as is the case for draw/bend tests and flanged channel forming) has been noted in several analyses [23,35–41]. However, until recently, the magnitude of the Bauschinger effect in sheet metal tension–compression [42,43] or bend/reverse bend [44,45] had seldom been measured because of the instability of metal sheets subjected to in-plane compression.

A variety of manufacturing techniques have been developed for dealing with springback. The simplest involves designing tools to over-bend the sheet to compensate for springback. However, this is not applicable to complex curved parts and, without additional control, this approach can lead to large variations in practice as material properties and thickness vary. Other approaches include the use of deformable tools [46,47], adjustments to small die radii and clearances [22,24], through-thickness deformation [48], variable or stepped blank holder force control [21,36,49–52], multiple forming steps [19,36,53], or reconfigurable tooling [54]. Each of these methods can benefit from accurate knowledge of springback from measurement and analysis.

The current work is motivated by a lack of systematic springback measurements for deformation under a range of carefully controlled laboratory conditions but applicable to industrial practice. In particular, the role of friction coefficient and R/t in springback has been equivocal, and data is needed to evaluate the accuracy of simulation techniques.

Table 1
Chemical compositions in weight percent [55,56]

Material	C	Mn	P	S	Si	Cu	Ni	Cr	Mo	Sn	Al	N	V	Cb
DQSK[55]	0.035	0.22	0.009	0.010	0.007	0.03	0.01	0.02	0.01	0.002	0.031	0.004	0.000	0.001
HSLA[55]	0.070	0.477	0.010	0.004	—	0.02	0.02	0.03	—	0.001	0.022	0.005	—	0.039
6022-T4[56]	Si—1.24		Fe—0.13		Cu—0.09		Mn—0.07		Mg—0.58		Ti—0.02			

2. Experimental procedure

Strain hardening curves, with particular attention to the low-strain region, were generated by standard tensile testing. Stretch/bend testing was conducted using apparatus and specimen procedures developed by Matlock and coworkers [32–34] for the measurement of friction. Digitizing of the specimen shapes and several forms of subsequent analysis were used to reveal the nature of the springback after removal from the grips of the device.

2.1. Materials

Three materials were selected and provided under the auspices of a large cooperative project to predict springback following automotive forming operations. The first alloy, DQSK steel [55], is a current mainstay of the automotive industry for body panels. The other two alloys are promising or planned alternatives suitable for reducing vehicle mass: HSLA steel [55], and 6022-T4 aluminum [56]. The HSLA steel was hot-dipped galvanized while the other materials were uncoated. Chemical compositions are listed in Table 1.

Standard tensile tests [57] were carried out using a 50 mm-gage extensometer to record strains, at a nominal strain rate of 0.001/s. Three stress–strain curves were averaged to produce a single composite set of data points for the rolling direction (parallel to the draw direction for all draw–bend tests) of each material. Constitutive equations were then produced from this set of data points, with special attention to the region near the elastic–plastic transition.

To describe the stress–strain curve accurately, three regions were defined. The first is a linear fit to the initial elastic region, the second is a elastic–plastic transition region, and the third is large strain plasticity. For the plastic region of the curve above 5% strain, typical hardening laws of the Hollomon [58], Swift [59], and Voce [60] types were considered. The Holloman law fit well for the steels and the Voce law fit well for 6022-T4. The transition zone was of particular interest for its effects on springback response and simulation. Therefore, the plastic laws were modified to include this region. A separate set of tensile tests involving repeated loading and unloading with data acquired at smaller strain intervals was used to fit the linear region to obtain Young's modulus.

To describe the transition region, the deviation of this portion of the curve from the large-strain fit was determined, such that the deviation automatically approached zero at large strain. Trial and error fits for various kinds of equations were employed to improve the curve fit in this region. Each of the equations was finally fit to the experimental curve over the entire strain range using a least-squares technique to obtain the final terms of the constitutive equations. The transition region and large-strain

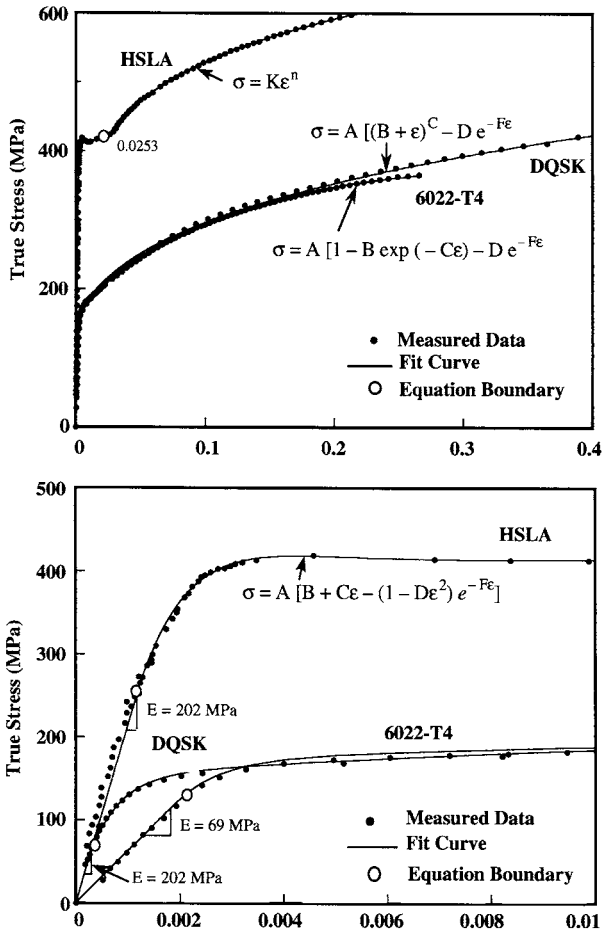

Fig. 1. Measured and fit strain hardening.

plastic regions of DQSK and 6022-T4 were combined without significant degradation of the fit and thus only two equations. The irregularity of the HSLA yield point curve required the use of three regions in the final fit. For each fit, an overall correlation coefficient greater than 0.99 was obtained. The resulting constitutive equations and the comparison with the composite experimental data appear in Fig. 1 and Table 2.

2.2. Draw/bend test

The draw/bend test [32–34] used in this study, Fig. 2, consists of two hydraulic actuators oriented 90° to one another, with a fixed or rolling cylinder at the intersection of their action lines to simulate a tooling radius over which the sheet metal is drawn. The upper actuator (horizontal) is programmed to provide a constant restraining force (or back force) while the lower actuator is set to displace at a constant speed, thus drawing the strip over the cylinder. The material undergoes tensile loading, bending, and unbending as it is drawn over the tooling. At the end of the test, the material is allowed

Table 2
Material properties and hardening laws, rolling direction tensile tests

Material σ_y: yield stress r_{RD}: plastic anisotropy, RD	Strain	Stress equation (c = correlation coefficient)	Constants
DQSK	$\varepsilon < 0.0035$	$\sigma = E\varepsilon$	$E = 212$ GPa
($t = 1.50$ mm) ($\sigma_y = 159$ MPa) ($r_{RD} = 1.87$)	$\varepsilon > 0.0035$	$\sigma = A[(B+\varepsilon)^C - De^{-F\varepsilon}]$ $c = 0.99983$	$A = 539$ MPa $B = 0.00965$ $C = 0.274$ $D = 0.278$ $F = 1700$
HSLA	$\varepsilon < 0.0012$	$\sigma = E\varepsilon$	$E = 202$ GPa
($t = 1.50$ mm) ($\sigma_y = 414$ MPa) ($r_{RD} = 0.69$)	$0.0012 < \varepsilon < 0.0253$	$\sigma = A[B + C\varepsilon - (1 - D\varepsilon^2)e^{-F\varepsilon}]$ $c = 0.99692$	$A = 592$ MPa $B = 0.686$ $C = 1.044$ $D = 109000$ $F = 995$
	$\varepsilon > 0.0253$	$\sigma = K\varepsilon^n$ $R = 0.99987$	$K = 772$ MPa $n = 0.163$
6022-T4	$\varepsilon < 0.002$	$\sigma = E\varepsilon$	$E = 69$ GPa
($t = 0.91$ mm) ($\sigma_y = 172$ MPa) ($r_{RD} = 0.73$)	$\varepsilon > 0.002$	$\sigma = A[1 - B\exp(-C\varepsilon) - De^{-F\varepsilon}]$ $c = 0.99992$	$A = 389$ MPa $B = 0.566$ $C = 8.44$ $D = 1.20$ $F = 1120$

to spring back by removal of the specimen from the grips of the fixtures. The parts of the strip outside the formed region remain straight.

Strips were sheared to lengths of 508 mm along the sheet rolling direction, with widths of 50 mm. After one end was gripped in the upper fixture, each strip was hand-formed to an unloaded radius of 90° (± approximately 1°), and the other end was clamped in the lower grip. The hand forming of the initial radius conforming to the tooling is a possible source of variation from test-to-test, although this formed region is small compared with the overall draw distance of 127 mm. For the central radius value of 9.5 mm, the ratio between the length of the two regions (one corresponding to a single bend and the other to a bend-and-unbend) is 9-to-1. For the high sheet tensions employed, these small variations will be essentially removed by plastic deformation throughout a large part of the sheet thickness as the strip originally formed to the radius passes through the rest of the contact region and then exits. Simulations of elastic–plastic pure bending corresponding to the hand forming operation show that the relief of all of the residual stresses results in an angular change less than 0.3°. Thus, it appears that the variations introduced by hand forming the initial radius are inconsequential compared with other sources of test variation such as load control, material property variation, and friction coefficient changes.

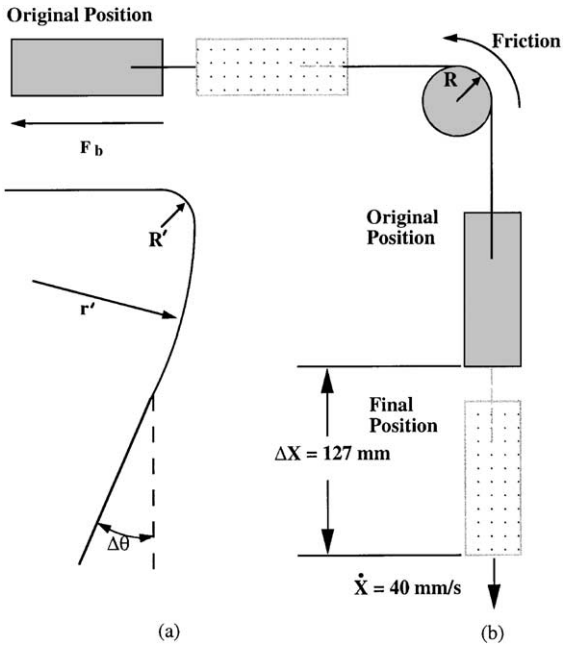

Fig. 2. Draw/bend test geometry: (a) specimen shape after unloading; and (b) original and final shapes during testing.

The strip was drawn over the radius at a constant velocity of 40 mm/s. After forming and removal, the shapes were traced onto paper; the traces being optically digitized later. Measurements were taken from both the traces and the digitized images. Gage marks applied to the outer surface (50 mm apart) were used for measurement of the axial strains.

Note. As part of quantifying day-to-day and test-to-test scatter, repeated measurements of $\Delta\theta$ were conducted over a period of time [61]. The results were consistent, within the measurement scatter, for both steels. For 6022-T4 aluminum, however, the springback angles continued to increase for periods up to several months after forming. A few tests of other aluminum alloys: 2008-T4, 5182-O, and 6111-T4, showed similar behavior, presumably related to room-temperature creep driven by the residual stress pattern. This was mainly observable for the conditions producing large $\Delta\theta$. The angles reported throughout this paper refer to the long-time measurements for 6022-T4.

In order to investigate the roles of tool radius, tension, and friction in springback, tests were conducted with a selection of these process parameters. Multiple sets of tooling, both fixed and rolling, were constructed with radii of 3.2, 6.4, 12.7, and 25.4 mm. Draw restraint (via back force) was set at a fraction of each material's yield strength in the following increments: 0.5, 0.7, 0.9, 1.1, 1.3 and 1.5. Friction was modified by using lubricated rollers (minimum friction), lubricated fixed tools (medium friction), and unlubricated fixed tools (high friction). A standard industrial drawing lubricant [62] was used for all lubricated cases.

The friction coefficient for each material and lubricant can be quantified by various analytical schemes [32,34] based on the front (measured) and back (controlled) forces for each test. Use

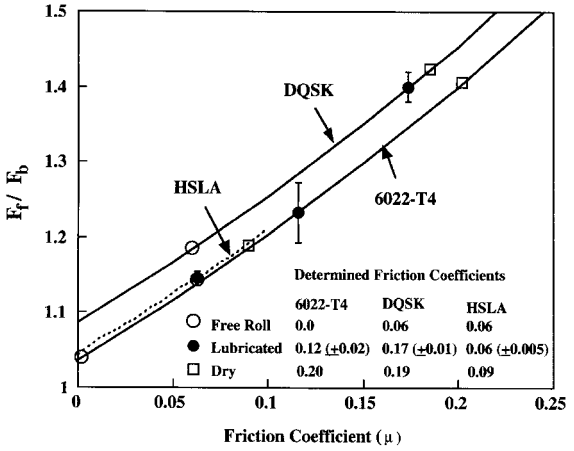

Fig. 3. Simulated force ratios as functions of friction coefficient, with superimposed experimental results.

of these schemes gave inconsistent results and, in some cases, values of friction coefficient outside of normally reported ranges. Instead, using a series of simulation techniques and elements, the draw/bend test was simulated [63–68]. By comparing simulated front forces with measured ones, Fig. 3, it was possible to obtain friction coefficients for each combination of material and lubrication condition. These results were nearly independent of the simulation details, and they have the advantage of incorporating actual conformance to the tool surface (rather than ideal conformance usually assumed), variable pressure throughout the tool contact, and bending/unbending terms in the draw force. The scatter shown in Fig. 3 for lubricated cases is calculated from the scatter of measured front and back forces for a single condition. The effective friction coefficients for DQSK and HSLA under free-rolling conditions are not as low as expected ($\mu = 0.06$), presumably because of rolling friction caused by bending of the roller under the higher draw loads required by these thicker materials. The unexpectedly low friction coefficient for the dry case for HSLA ($\mu = 0.09$) may be related to the lubricity of the coating for that material. The other two materials were uncoated.

Triplicate testing of all process combinations (comprising 648 experiments) was judged impractical, so a more limited series was devised to reveal the main features. The central combination, the one considered most typical of industrial practice, consisted of lubricated, fixed tooling, a normalized tensile force ($\overline{F}_b$) 0.9 and 1.1 times the yield strength, and a tooling radius of 9.5 mm. This radius is a common one in automotive dies [69].

From this central combination, a series of tests was performed at various R/t or F_b while maintaining the other variables constant. These are the principal combinations used to determine the experimental sensitivity of springback to R/t and F_b. The extreme combinations of these variables were also tested, although in some cases material or machine limitations intervened. HSLA failed for $\overline{F}_b$ greater than 1.1 of the yield strength, and the smallest tool radius did not allow rolling during drawing, presumably because of roller bending, so reliable low friction conditions could not be obtained. Because of the observed difficulties in obtaining low-friction conditions in some of these cases, the results for low-friction conditions should be considered approximate for the smaller tool radii. A complete set of test results for all tested combinations appears in Tables 3–5.

Table 3
Measured forces, strains, curvatures and springback angles from draw/bend tests of 6022-T4 aluminum alloy[a]

R (mm)	$\overline{F_b}$	F_b (N)	F_f (N)	$\Delta\theta$ (degrees)	$\Delta\theta_1$ (degrees)	$\Delta\theta_2$ (degrees)	ε_l	R_a (mm)
Dry								
6.35	0.9	6841	9056	9.8	−7.9	17.7	0.082	213
9.525	0.5	3807	5413	47.7	−7.0	54.7	0.038	1267
9.525	0.7	5329	7272	24.7	−6.5	31.2	0.059	556
9.525	0.9	6899	9701	5.1	−6.5	11.6	0.065	236
9.525	1.1	8416	11347	3.6	−3.7	7.3	0.103	269
12.7	0.9	6877	9145	2.2	−5.6	7.8	0.050	244
Lubricated								
3.175	0.5	3060	2566	79.2	−10.2	89.4	0.085	1509
3.175	0.5	3732	2949	70.8	−16.6	87.4	0.097	1247
3.175	0.9	6881	9532	17.5	−5.1	22.6	0.137	284
3.175	1.1	8371	11360	5.4	−1.6	7.0	0.217	556
6.35	0.9	6917	8900	10.5	−6.8	17.3	0.085	224
6.35	1.1	8451	10622	6.3	−7.8	14.1	0.113	234
6.35	1.1	8981	11467	2.6	51.2	−48.6	0.223	996
9.525	0.5	3879	5186	52.2	−9.9	62.1	0.058	998
9.525	0.7	5369	6814	35.8	−9.5	45.3	0.064	729
9.525	0.9	6926 ± 22	8669 ± 67	6.9 ± 0.5	−8.5 ± 2.8	15.4 ± 2.8	0.079 ± 0.055	221 ± 10
9.525	0.94	7179 ± 9	8714 ± 209	5.2 ± 0.3	−8.0 ± 0.8	13.2 ± 1.1	0.042 ± 0.016	218 ± 8
9.525	1.1	8420	10328	4.6	−7.4	12.0	0.063	213
9.525	1.3	9861	12036	3.2	−6.2	9.4	0.065	290
9.525	1.4	10546	12739	0	−4.8	4.8		572
12.7	0.9	6952 ± 49	8513 ± 22	5.3 ± 0.6	−5.7 ± 1.4	10.9 ± 2.0	0.124 ± 0.052	249 ± 8
12.7	1.1	8500 ± 71	10168 ± 49	3.6 ± 0.6	−4.5 ± 4.8	8.1 ± 5.3	0.070 ± 0.008	251 ± 23
25.4	0.9	9439	10444	1	−10.6	11.6		274
25.4	1.1			−0.4	−3.0	2.6	0.061	246
Free rolling								
2.38125	0.3	2224	4524	81.7	−6.9	88.6	0.061	1725
2.38125	0.5	3763 ± 13	6374 ± 245	63.5 ± 4.5	−11.7 ± 5.4	75.1 ± 9.8	0.095 ± 0.044	1354
2.38125	0.9	6797	9279	17.9	−15.9	33.8	0.062	450
3.175	0.5	3794 ± 22	6067 ± 53	71.1 ± 2.9	−2.8 ± 3.4	73.9 ± 2.0	0.095 ± 0.005	1554 ± 218
6.35	0.5	4114 ± 0	4924 ± 31	63.4 ± 3.4	−13.3 ± 2.8	76.7 ± 0.6	0.092 ± 0.029	1651 ± 56
6.35	0.9	7264	8349	30.6	−6.2	36.8	0.007	795
6.35	1.4	10640 ± 62	12107 ± 231	4.1 ± 0.5	−1.6 ± 2.4	5.7 ± 1.9	0.157 ± 0.043	391 ± 69
6.35	?	10840	12365	2.4	−1.2	3.6	0.043	533
9.525	0.5	3848	4154	57.8	−8.5	66.3	0.060	1458
9.525	0.7	5329	5627	45.6	−7.9	53.5	0.012	1186
9.525	0.9	6957	7237	33.3	−7.5	40.8	0.054	892
9.525	1.1	8758	8852	11.1	−7.2	18.3	0.055	394
9.525	1.4	10751	11182	5	−7.1	12.1	0.047	328
12.7	0.9			25.6	−5.4	31.0	0.011	
25.4	0.5	3856 ± 9	3892 ± 9	35.9 ± 2.4	−14.8 ± 1.5	50.7 ± 3.9	0.131 ± 0.046	2487 ± 168
25.4	0.9	7103	7157	9.2	−8.3	17.5	0.015	490
25.4	1.4	10684 ± 4	10693 ± 9	−0.6 ± 0.4	−6.3 ± 1.5	5.7 ± 1.7	0.081 ± 0.078	330 ± 5

[a] R: Tool radius, $\overline{F_b}$: normalized back force, F_b: actual back force, F_f: actual front force, ε_l: longitudinal strain in the curl region and R_a: anticlastic curvature in the curl region.

Table 4
Measured forces, strains, curvatures and springback angles from draw/bend tests of DQSK[a]

R (mm)	$\overline{F_b}$	F_b (N)	F_f (N)	$\Delta\theta$ (degrees)	$\Delta\theta_1$ (degrees)	$\Delta\theta_2$ (degrees)	ε_l	R_a (mm)
Dry								
6.35	0.9	10715	16102	4.1	−4.3	8.4	0.099	881
9.525	0.5	5943	9345	7.3	−6.6	13.9	0.053	897
9.525	0.7	8371	12245	5.5	−4.3	9.8	0.065	770
9.525	0.9	10760	15323	4	−1.7	5.7	0.075	861
9.525	1.1	13322	18450	1.5	−2.5	4.0	0.091	1288
12.7	0.9	10746	16231	3.2	−4.4	7.6	0.062	876
Lubricated								
3.175	0.9	10724	18259	−5.4	7.5	−12.9	0.182	3119
3.175	1.1	13202 ± 125	20181 ± 165	−5.1 ± 0.9	−16.0 ± 12.3	10.9 ± 11.4	0.219 ± 0.009	1857 ± 295
6.35	0.9	10786	15688	4.6	−6.3	10.9	0.101	892
6.35	1.1	13193	18130	2.6	−3.4	6.0	0.116	925
9.525	0.5	5885	9287	7.2	−3.2	10.4	0.039	1148
9.525	0.5	6272	9599	7.9	−1.8	9.7	0.040	1267
9.525	0.7	8402	12276	7.3	0.1	7.2		
9.525	0.9	10809 ± 9	15123 ± 165	5.6 ± 0.5	−1.4 ± 2.2	6.9 ± 2.4	0.069 ± 0.005	988 ± 81
9.525	1.1	13233	17730	3	−4.6	7.6	0.085	955
9.525	1.3	15608	20358	2.2	−3.4	5.6	0.112	927
9.525	1.5	17930	21880	0.5	−3.1	3.6	0.154	2162
12.7	0.9	10813 ± 31	13375 ± 147	6.2 ± 0.9	−2.7 ± 1.5	8.8 ± 0.6	0.063 ± 0.010	823 ± 81
12.7	1.1	13268	15746	4.8	2.1	2.7	0.061	927
12.7	1.1	12819	15323	3.6	−2.1	5.7	0.071	925
25.4	0.9	10826	13295	2.8	−3.0	5.8	0.030	676
25.4	0.9	11124	13838	2	−3.8	5.8	0.033	729
25.4	1.1	13237	17365	0.3	−1.4	1.7	0.054	732
25.4	1.1	13219	17116				0.040	737
Free rolling								
3.175	0.5	5934 ± 13	13175 ± 338	−3.8 ± 0.1	−17.2 ± 0.8	13.4 ± 0.9	0.118 ± 0.003	1417 ± 130
6.35	0.5	5974	9554	8.4	−7.3	15.7	0.057	1125
6.35	0.5	6258	9839	7.5	−5.3	12.8	0.064	1130
6.35	0.5	6730	10319	7	−6.8	13.8	0.061	1201
6.35	0.9	11093	14981	5.7	−8.2	13.9	0.098	1250
6.35	1.5	18130 ± 22	22569 ± 133	−0.1 ± 0.1	−7.6 ± 0.4	7.5 ± 0.6	0.183 ± 0.002	2367 ± 8
9.525	0.5	5987	7766	9.4	−6.7	16.1	0.036	1115
9.525	0.7	8358	10052	7.8	−4.3	12.1	0.053	1290
9.525	0.9	10795	12806	7.1	−4.5	11.6	0.061	998
9.525	1.1	13455	14905	3.2	−5.0	8.2	0.106	1346
9.525	1.5	17974	20870	0.7	−1.1	1.8	0.135	2014
12.7	0.9	10773	12188	5.7	−4.9	10.6	0.050	803
25.4	0.5	5996 ± 13	6485 ± 13	7.0 ± 0.5	−4.7 ± 1.0	11.7 ± 1.5	0.012 ± 0.005	886 ± 198
25.4	0.9	10947	11307	4	−4.2	8.2	0.024	688
25.4	1.5	18014 ± 9	18428 ± 27	−0.4 ± 0.0	−3.6 ± 0.2	3.2 ± 0.2	0.069 ± 0.006	767 ± 18

[a] R: Tool radius, $\overline{F_b}$: normalized back force, F_b: actual back force, F_f: actual front force, ε_l: longitudinal strain in the curl region and R_a: anticlastic curvature in the curl region.

Table 5
Measured forces, strains, curvatures and springback angles from draw/bend tests of HSLA[a]

R (mm)	$\overline{F_b}$	F_b (N)	F_f (N)	$\Delta\theta$ (degrees)	$\Delta\theta_1$ (degrees)	$\Delta\theta_2$ (degrees)	ε_l	R_a (mm)
Dry								
6.35	0.9	28169	34205	0.6	−15.5	16.1	0.191	3254
9.525	0.5	15759	20470	16.6	−5.6	22.2	0.070	993
9.525	0.9	28214	33582	0.9	−7.4	8.3	0.126	1643
12.7	0.9	28280 ± 4	33556 ± 298	1.7 ± 0.6	−4.6 ± 1.3	6.3 ± 1.9	0.094 ± 0.007	897 ± 76
Lubricated								
3.175	0.7	21826	29268	−8.3	−15.3	7.0	0.235	3035
6.35	0.9	28205	33018	−0.2	−7.9	7.7	0.167	1151
6.35	1	31332	35571	0	−4.8	4.8	0.208	2667
9.525	0.5	15572	19745	14	−7.2	21.2	0.063	874
9.525	0.7	23179	27400	7.9	−4.1	12.0	0.089	894
9.525	0.9	28231 ± 178	32337 ± 173	2.6 ± 0.7	−5.5 ± 1.6	8.0 ± 1.8	0.117 ± 0.003	1057 ± 79
9.525	1	31407	34930	0.9	−7.1	8.0	0.152	1377
9.525	1.02	32021	35379	0.8	−6.8	7.6	0.152	1425
9.525	1.04	32399	36318	0.6	−5.5	6.1	0.172	1923
9.525	1.04	32671	36144	0	0.0	0.0	0.211	2225
12.7	0.5	15644	19380	11.8	−5.8	17.6	0.044	693
12.7	0.9	28356	32088	0.9	−4.9	5.8	0.093	622
12.7	1	31447	34494	0.8	16.7	−15.9	0.127	884
12.7	1.02	32057	35050	0.8	−4.3	5.1	0.135	859
12.7	1.04	33284	36371	0.5	2.3	−1.8		
25.4	0.9	28409	31065	−0.7	−3.7	3.0	0.045	632
25.4	1	31519	34170	−1.2	−3.1	1.9	0.061	759
Free rolling								
6.35	0.5	15741 ± 27	20977 ± 67	13.5 ± 0.7	−8.5 ± 3.1	22.1 ± 3.5	0.094 ± 0.003	818 ± 25
6.35	0.9	28191	33627	0.7	−2.6	3.3	0.169	
6.35	1.04	31492	37310	0.8	−7.1	7.9	0.260	1636
9.525	0.5	15764	17836	11.5	−9.6	21.1	0.058	859
9.525	0.7	22018	24331	9.8	−7.7	17.5	0.083	922
9.525	0.9	28289	32390	1.9	−7.8	9.7	0.118	1603
9.525	1	31421	34009	2	−2.9	4.9	0.137	2878
9.525	1.02	31937 ± 44	35895 ± 36	0.8 ± 0.2	−4.5 ± 2.8	5.3 ± 3.0	0.168 ± 0.004	3193 ± 84
12.7	0.9	28414	29628	3.4	−1.6	5.0	0.076	838
25.4	0.5	15839	16471	13.7	−8.7	22.4	0.022	917
25.4	0.9	28400	28841	2.1	−4.4	6.5	0.045	693

[a] R: Tool radius, $\overline{F_b}$: normalized back force, F_b: actual back force, F_f: actual front force, ε_l: longitudinal strain in the curl region and R_a: anticlastic curvature in the curl region.

2.3. Measurement of springback

The final specimen shape can be defined by two radii of curvature, R' and r' (see Fig. 2), and two corresponding angles, θ_1 and θ_2. R' and θ_1 are the unloaded quantities representing the region

remaining in contact with the tool at the end of the test (before unloading), which has undergone only bending, not straightening. r' and θ_2 represent the region which has been drawn over the tool and which has undergone bending and straightening. The two measures are related by fixed arc lengths of $R\pi/2$ (tool contact length) and 127 mm (the driving actuator displacement), respectively. The springback angles are the changes of these measures upon unloading:

$$\Delta\theta_1 = \theta_1 - \theta_1^{\text{loaded}} = \theta_1 - \pi/2 = \pi/2\ (R/R' - 1), \tag{1}$$

$$\Delta\theta_2 = \theta_2 - \theta_2^{\text{loaded}} = \theta_2 - 0^\circ = 127\ \text{mm}/r', \tag{2}$$

$$\Delta\theta = \Delta\theta_1 + \Delta\theta_2. \tag{3}$$

The change of θ_1 ($\Delta\theta_1$ is generally negative) represents relaxation from a single bend to conform to the tool radius while θ_2 corresponds to a region of straightening from this radius. $\Delta\theta_2$, generally positive, is a measure of "sidewall curl" [70,71] in industrial channel forming.

The shapes of the samples were carefully traced onto paper immediately after unloading. (For 6022-T4, the shapes were retraced at long times, and these long-time shapes are reported here.) θ was measured directly from the traces by constructing straight lines through the specimen legs. The overall springback angle θ (or $\Delta\theta$) determined from CAD image and tracing were first compared, and were found to agree to a typical tolerance of 0.2°. Because of the large draw distance involved in the draw/bend test, the strains occurring during springback can be resolved with high precision. The measurement scatter of 0.2° corresponds to a strain resolution at the outer fiber of the sidewall curl area of 0.00001 or 0.001%.

Several techniques were tested to obtain the component angles θ_1 and θ_2. The most consistent was based on the use of digitized images and CAD software. A circle was numerically fit to an arc length of $(\pi/2)R$ in the single-bend region. This circle was superimposed digitally, and the tangent points with both the upper leg and curl region were determined (separated by a fixed arc length of $(\pi/2)R$). The tangent at the tool radius/curl boundary defines both θ_1 and θ_2. Comparison of angles determined by this procedure for multiple experiments under identical conditions revealed that typical measurement uncertainties for θ_1 and θ_2 (or $\Delta\theta_1$ and $\Delta\theta_2$) are 1°–3°, the larger errors corresponding to smaller tool radii. Therefore, the measurement of $\Delta\theta$ is more accurate than its components by an order of magnitude.

For certain test results, principally aluminum specimens with intermediate sidewall curling, a secondary curvature in the sidewall curl region orthogonal to the principal curvature could be observed. This secondary curvature, which occurs as a result of differential contraction in the width direction from the top to bottom sides of the strip, is known as anticlastic curvature [1] [7,72]. The existence of the persistent secondary curvature during unloading increases the effective moment of inertia of the cross section about the bending axis, thus reducing the springback angle. The anticlastic curvature was measured on each specimen at a position 51 mm from the location of the boundary between the straight upper leg and first curve (76 mm for the test cases of tool radii of 25.4 mm), thus near

[1] It should be noted that the principal and secondary curvature in the sidewall curl region are typically both concave on the tool side of the strip, which violates the formal definition of "anticlastic", although this term has acquired the meaning of a secondary, orthogonal curvature resulting from a primary bending.

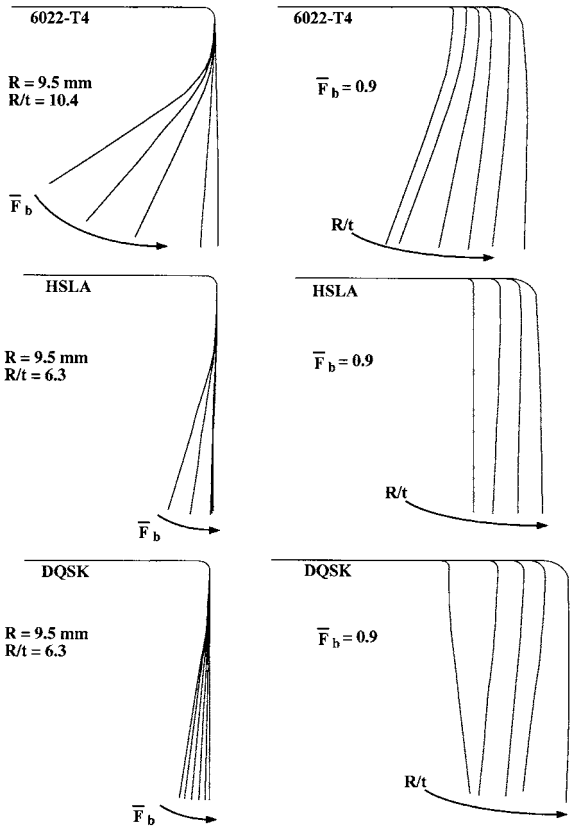

Fig. 4. Typical final specimen shapes for variation of back force ($R = 9.5$ m) and tool radius ($\overline{F}_b = 0.9$).

the center of the sidewall curl region. The arc height at the center of the strip (h) and width of the section (w) were measured and the radius of curvature (R_a) was computed as follows:

$$R_a = \frac{1}{\kappa} = \frac{h}{2} + \frac{w^2}{8h}, \tag{4}$$

where κ is the curvature. The measured anticlastic curvatures are presented in Tables 3–5.

3. Results

Typical shapes of the unloaded strips are presented in Fig. 4. As expected, sheet tension has a clear and dramatic effect on reducing total springback. (The back force is presented in normalized form by dividing the measured back force by the force to yield the material in tension, as presented for each material in Table 2.) The role of increasing R/t (for a normalized back force of 0.9) is less consistent, with a significant decrease of $\Delta\theta$ for 6022-T4 and little measurable effect for HSLA. For DQSK, only the extreme values of R/t have a significant effect, including a reverse sidewall curl at the smallest R/t tested (2.1), a trend reported by others for drawing steel and channel forming [11,22,24].

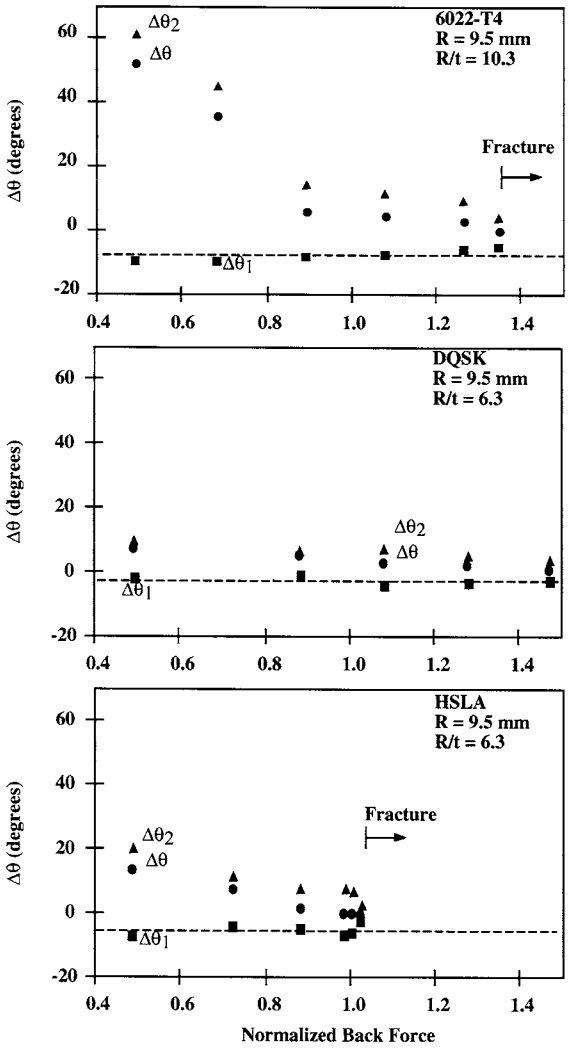

Fig. 5. Variation of total component ($\Delta\theta_1$, $\Delta\theta_2$) and total springback angles ($\Delta\theta$) with back force.

Figs. 5 and 6 show the relationship of total springback angle ($\Delta\theta$) to its components: $\Delta\theta_2$ (corresponding to sidewall curl springback) and $\Delta\theta_1$ (corresponding to springback over the die radius). For the three tested materials, $\Delta\theta_1$ is small and approximately constant while $\Delta\theta_2$ changes markedly with the level of back force. In terms of R/t, $\Delta\theta_1$ is slightly sensitive for 6022-T4 (Fig. 6), but no trend could be observed outside of the scatter. The variation of overall shape is thus dominated by the sidewall curl, as would be expected for the large draw distance (sidewall curl length) relative to the tool contact length. Because of the much better precision available for measuring $\Delta\theta$ compared to $\Delta\theta_1$ or $\Delta\theta_2$, the remainder of the results will be presented in terms of $\Delta\theta$, although all three angles are available in Tables 3–5 for detailed comparisons with theory or simulation.

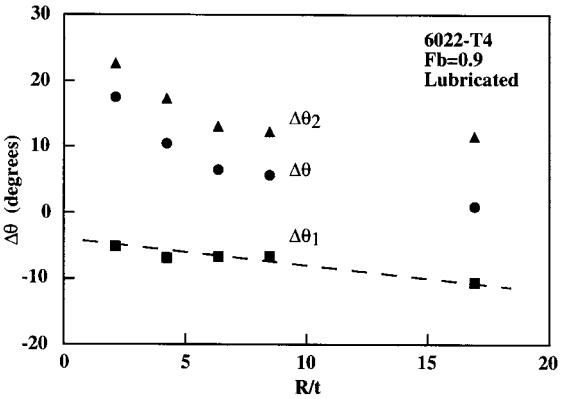

Fig. 6. Variation of springback angle with the radius of tool-to-sheet thickness (R/t).

The test-to-test scatter of measured angles was investigated by repeating tests of the central conditions ($\overline{F}_b = 0.9, R = 9.5$ mm, lubricated) at least seven times over several days. The standard deviation of the experimentally determined springback angle (θ or $\Delta\theta$) was 0.5° for DQSK, 1.1° for 6022-T4, and 0.7° for HSLA. The magnitude of test-to-test scatter correlates approximately with the magnitude of the springback. For comparison, the scatter in measurement of $\Delta\theta$ (from a single experiment) is approximately 0.2°, while the scatter of the two component angles, $\Delta\theta_1$ or $\Delta\theta_2$, is 1–3°.

Fig. 7 shows the expected trend of decreasing springback with back force (or sheet tension), as reported in virtually every reported analytical and experimental study. While DQSK and HSLA show a continuously decreasing springback, 6022-T4 shows a plateau for normalized back force greater than 0.9. This plateau of springback at higher sheet tensions has been reported by others [14,43].

Fig. 7 also shows that friction in normal industrial ranges (i.e. well-lubricated to dry conditions) has no measurable effect on springback. Even for the free-rolling condition, corresponding to the minimum friction attainable, only the 6022-T4 showed a significant difference from the lubricated/dry tests, mainly at intermediate back forces. Experimental results in the literature correlate springback to friction conditions. However, in most such experiments or forming operations, the back force is not controlled independently, as it is for the present experiments. The discrepancy in results suggests that the role of friction in practical forming lies in the modification of sheet tension.

Tooling radius has a modest effect on springback, Figs. 8 and 9. For back forces less than the yield force, increasing R/t beyond 5 reduces springback for both 6022-T4 and DQSK. There are few data for R/t less than 5, but the trend reverses, with springback approaching zero as R/t approaches 2. This trend is consistent with reported observations [18,22,24], and the critical ratio of 5–6 is generally taken as the boundary between bending of thin and thick shells [6]. For large back forces, and for all HSLA results, R/t has little or no effect on springback. These results suggest that for low hardening induced during bending (i.e. for HSLA or at high sheet tension), the effect of R/t is diminished.

The measured anticlastic curvature (κ_a) for 6022-T4 increases dramatically for normalized back forces in the range of 0.8–1.2, Fig. 10a. For $R/t < 7$, the critical range is narrower, perhaps $\overline{F}_b =$ 0.9–1.0. In either case, as the sheet tension approaches the yield stress, persistent and significant anticlastic curvature is measured. For this range of back force, where the anticlastic curvature is large,

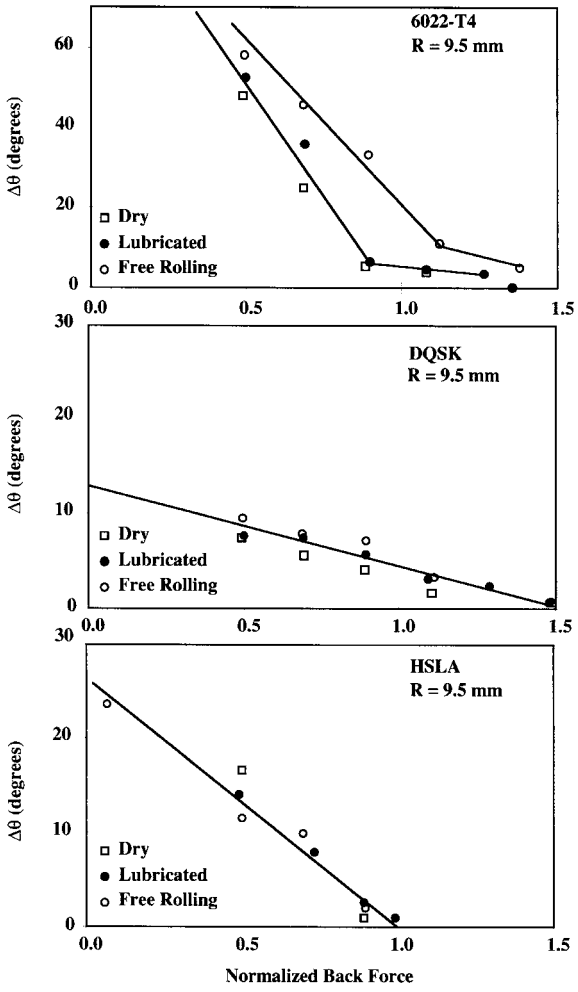

Fig. 7. Role of friction on measured total springback angle ($\Delta\theta$).

the springback angle drops precipitously, Fig. 5a. This correlation can be understood by considering the moment of inertia of the deformed strip of 50.8 mm width. This moment controls the principal bending and unbending. Three cases illustrate the range of moment of inertia (I) for a flat sheet (ideal two-dimensional case) of width 50.8 mm, a sheet with curvature of 0.001 mm^{-1} (for $\overline{F}_b < 0.9$ or $\overline{F}_b > 1.2$), and a sheet with curvature of 0.004 mm^{-1} (for $0.8 < \overline{F}_b < 1.2$). These values may be computed using standard formulas [73].

$$I(\kappa_a = 0.0\ \text{mm}^{-1}, R_a = \infty) = 3.2\ \text{mm}^4, \tag{5}$$

$$I(\kappa_a = 0.001\ \text{mm}^{-1}, R_a = 1000\ \text{mm}) = 3.6\ \text{mm}^4, \tag{6}$$

$$I(\kappa_a = 0.004\ \text{mm}^{-1}, R_a = 250\ \text{mm}) = 10.0\ \text{mm}^4. \tag{7}$$

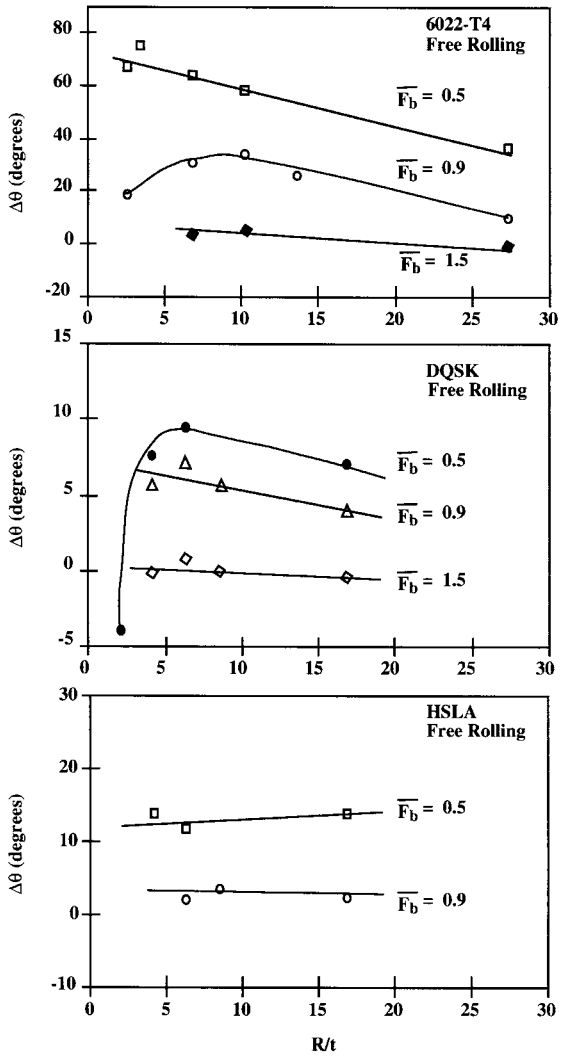

Fig. 8. Variation of total springback angle ($\Delta\theta$) with R/t ratio (free rolling condition).

Thus, anticlastic curvature has at most a modest effect on the section moment of inertia outside of the range of critical back forces, contributing 13% or less to the moment of inertia. In the critical region of R/t, the anticlastic curvature increases the flat-sheet moment of inertia by a factor of 3, thus potentially reducing springback by a similar factor. This analysis agrees with the trends in the measured springback values shown in Fig. 5a.

The anticlastic curvature for the thicker ($t = 1.5$ mm) DQSK and HSLA steels is much lower, Figs. 10b and c. It is nearly constant, within experimental scatter, over the range of back forces and R/t values tested. For comparison, the moment of inertia for these thicker sections is increased less than 5% by the typical anticlastic curvature of 0.001 mm^{-1} ($R_a = 1000$ mm). For the highest observed anticlastic curvatures for steels ($\kappa = 0.015\ mm^{-1}$, $R_a = 667$ mm), the increase of section

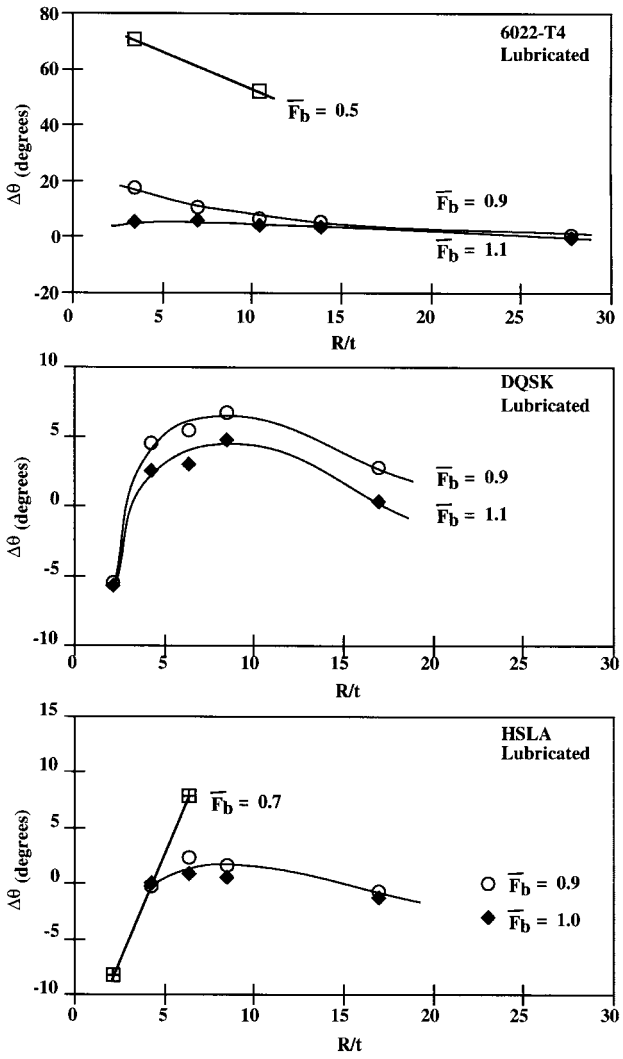

Fig. 9. Variation of springback angle with R/t ratio (lubricated condition).

moment of inertia is 11%. Thus, the steels are expected to show a smoothly decreasing springback with back force, as is the case in the measured values presented in Figs. 5b and c.

Fig. 11 illustrates the rapid change of the ratio of springback (primary) curvature-to-anticlastic (secondary) curvature with back force for 6022-T4. For $\overline{F}_b < 0.8$, the primary curvature is much greater than the anticlastic curvature (up to a ratio approaching 20). For $\overline{F}_b > 0.8$, the ratio reverses, and changes at a much lower rate.

4. Conclusions

Draw-bend tests have been conducted and analyzed to investigate the role of typical process variables on springback and to provide accurate data for evaluation of springback models and simulations

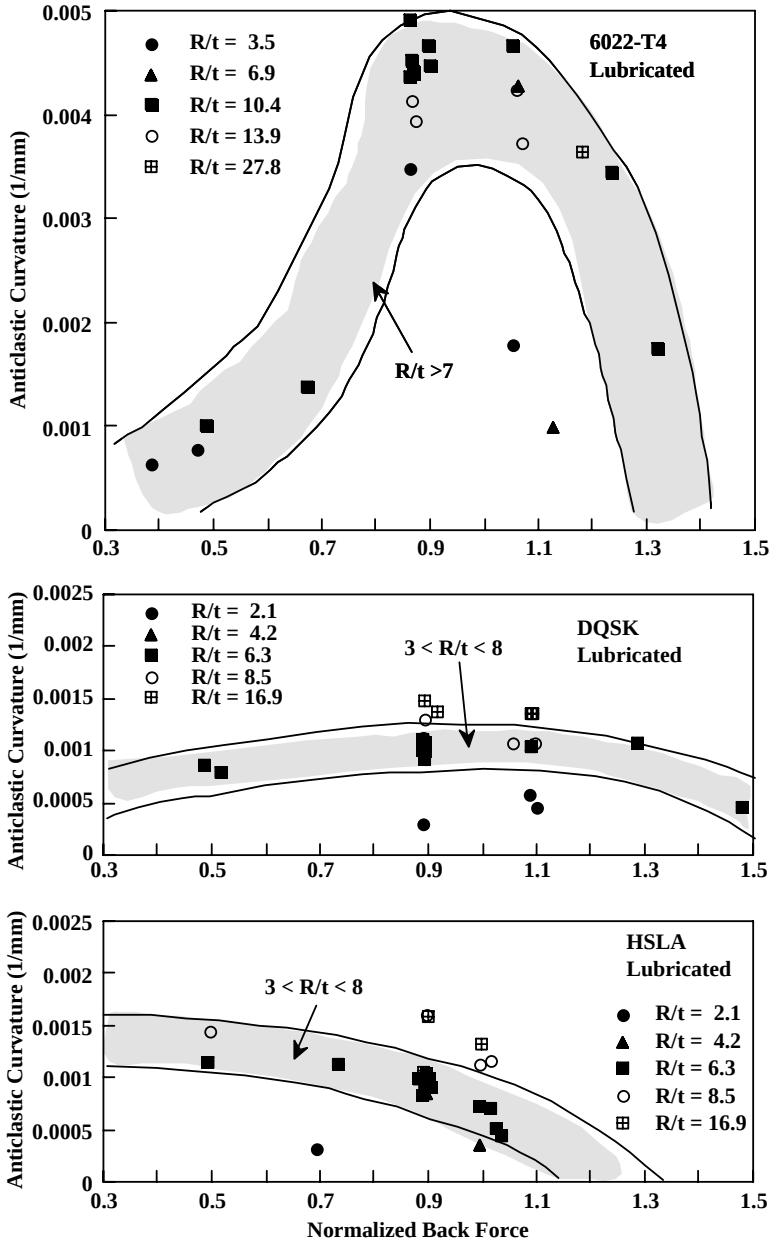

Fig. 10. Variation of measured anticlastic curvature with normalized back force.

of three sheet alloys: DQSK and HSLA steels, and 6022-T4 aluminum alloy. The following conclusions were reached:

1. The shape change associated with simple bending springback is much smaller than that associated with sidewall curl because of the extent of the affected area. The remaining conclusions are derived from overall shape change, which is dominated by sidewall curl.

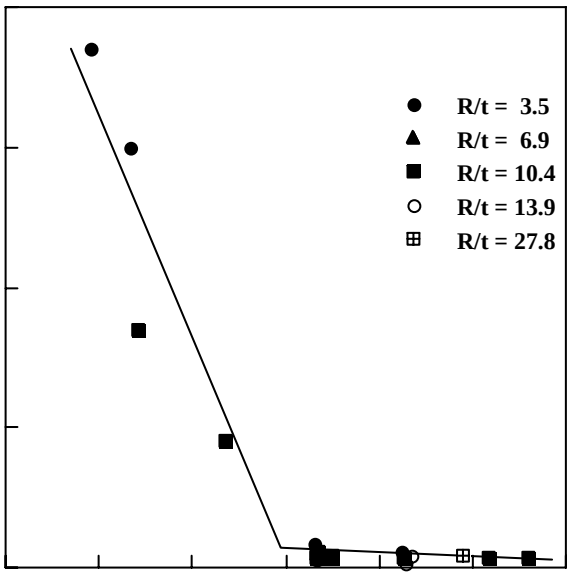

Fig. 11. Variation of primary-to-anticlastic curvature with normalized back force for 6022-T4 aluminum.

2. As consistently reported in the literature, applied tension drastically reduces springback, although an unexpected drop and plateau region of smaller dependence appears for back forces in the range of 0.8–1.2 times the material yield stress.
3. For 6022-T4, the rapid drop of springback angle at back forces near yield corresponds to the sudden increase of persistent anticlastic curvature. This appears to be the first measurement of persistent anticlastic curvature in connection with springback, and its correlation with process variables.
4. Friction in the range normally encountered in sheet forming practice has little effect on springback, although very low friction conditions increase springback for 6022-T4. This conclusion differs from some results appearing in the literature [13], presumably because for many experiments the sheet tension cannot be controlled independently of friction, as with the current one.
5. Springback decreases for larger tool radii (R/t greater than about 5). This result is in agreement with some of the literature [20] and is contrary with other reports [26]. For the steels, an inflection occurs for R/t near 5, and the trend reverses, with trends toward zero springback for R/t approaching 2. This trend agrees with reports in the literature [18,22,24]. There appears to be an opportunity of reducing springback by using very small tool radii.

Acknowledgements

We would like to thank the support of National Institute of Science and Technology for an Advanced Technology Project under the auspices of PNGV, CAMMAC (Center for Advanced Materials and Manufacturing of Automotive Components), and Dr. Kaiping Li for helpful discussions.

References

[1] Schroeder W. Mechanics of sheet-metal bending. Transactions of the American Society for Mechanical Engineers 1943;65:817–27.
[2] Sachs G. Principles and methods of sheet metal fabricating, vol. 100. New York: Reinhold Publishing Corp., 1951.
[3] Levy BS. Empirically derived equations for predicting springback in bending. Journal of Applied Metalworking 1984;3:135–41.
[4] Nadai A. Theory of flow and fracture of solids, vol. 1. New York: Ronald, McGraw-Hill, 1950.
[5] Phillips A. Introduction to plasticity. New York: Ronald, 1956.
[6] Huang M, Gerdeen JC. Springback of doubly curved developable sheet metal surface. Analysis of Autobody Stamping Technology, Society of Automotive Engineers 1994;103:125–38.
[7] Yu TX, Zhang LC. Plastic bending, theory and applications. Singapore: World Scientific, 1996.
[8] Yu TX, Johnson W. Cylindrical bending of metal strips. Material Technology 1983;10:439–47.
[9] Yuen WY. Springback in the stretch-bending of sheet metal with non-uniform deformation. Journal of Materials Processing Technology 1990;22:1–20.
[10] Sanchez L. RD, Robertson JC. Gerdeen Springback of sheet metal bent to small radius/thickness ratios. SAE Paper 960595, Warrendale, PA, Society of Automotive Engineers, 1996.
[11] Sudo C, Kojima M, Matsuoka T. Some investigations on elastic recovery of press formed parts of high.... Eighth Biennial Congress of IDDRG, 1974. p. 192–202.
[12] Chakhari ML, Jalinier JN. Springback of complex parts. Thirteenth Biennial Congress of IDDRG, 1984. p. 148–59.
[13] Hino R, Goto Y, Shirashi M. Springback of sheet metal laminates subjected to stretch bending and the subsequent unbending. Advanced Technology of Plasticity 1999;II:1077–82.
[14] Zhang ZT, Hu SJ. Mathematical modeling in plane strain bending. SAE Technical Publication No. 970439. Society of Automotive Engineers, 1997.
[15] Wang NM. Predicting the effect of die gap on flange springback. Proceedings of the 13th Congress of the IDDRG. Melbourne, Australia, 1984. p. 133–47.
[16] Kuwabara T, et al. 2-D springback analysis for stretch-bending processes based on total strain theory. Automotive Stamping Technology, SP-1067, SAE paper 950691. Warrendale, PA: Society of Automotive Engineers, 1995. 1–10.
[17] Ueda M, Ueno M, Kobayashi M. A study of springback in the stretch bending of channels. Journal of Mechanics Working Technology 1981;5:163–79.
[18] Davies RG. Sidewall curl in high-strength steels. Journal of Applied Metalworking 1984;3:120–26.
[19] Ayres RA. SHAPESET: a process to reduce sidewall curl springback in high strength steel rails. Journal of Applied Metalworking 1984;3:2:127–34.
[20] Bayraktar E, Altintas S. Square cup deep drawing and 2d-draw bending analysis of Hadfield steel. Journal of Materials Processing Technology 1996;60:183–90.
[21] Schmoeckel D, Beth M. Springback reduction in draw-bending process of sheet metals. Annals of the CIRP 1993;42:1:339–42.
[22] Hayashi Y. Analysis of surface defects and side wall curl in press forming. IDDRG 13th Biennial Congress, 1984. p. 565–80.
[23] Pourboghrat F, Chu E. Springback in plane strain stretch/draw sheet forming. International Journal of Mechanical Sciences 1995;36:3:327–41.
[24] Umehara Y. Technologies for the more precise press-forming of automobile parts. Journal of Materials Processing Technology 1990;22:239–56.
[25] Makinouchi AE, Nakamachi E, Onate, Wagoner RH, editors. NUMISHEET '93. The Institute of Physical and Chemical Research, 1993.
[26] Nine HD. In: Koistnen DP, Wang N-M, editors. Drawbead forces in sheet metal forming. Mechanics of sheet metal forming. New York: Plenum, 1978. p. 179–211.
[27] Nine HD. The applicability of Coulomb's law to drawbeads in sheet metal forming. Journal of Applied Metalworking 1982;2:200–10.
[28] Nine HD. In: Wagoner RH, editor. Testing lubricants for sheet metal forming, novel techniques in metal deformation testing. The Metallurgical Society of AIME, Warrendale, PA, 1983. p. 31–46.

[29] Wang NM. A mathematical model of drawbead forces in sheet metal forming. Journal of Applied Metalworking 1982;2:193.
[30] Liu YC. The effect of restraining force on shape deviations in flanged channels. American Society for Mechanical Engineers—Journal of Engineering and Material Technology 1988;110:389–94.
[31] Kuwabara T, Takahashi S, Ito K. Springback analysis of sheet metal subjected to bending–unbending under tension Part II (experimental verification). Advanced Technology of Plasticity. In: Altan T, editor. Proceedings of the 5th ICTP, vol. II. Columbus, Ohio, 1996. p. 747–50.
[32] Wenzloff GJ, Hylton TA, Matlock DK. A new procedure for the bending under tension friction test. Journal of Material Engineering and Performance 1992;1:5:609–13.
[33] Haruff JP, Hylton TA, Matlock DK. Frictional response of electrogalvanized sheet steels. The physical metallurgy of zinc coated steel. The Minerals, Metals and Materials Society 1993.
[34] Vallance DW, Matlock DK. Application of the bending-under-tension friction test to coated sheet steels. Journal of Material Engineering and Performance 1992;1:5:685–93.
[35] Baba A, Tozawa Y. Effect of tensile force in stretch-forming process on the springback. Bulletin of JSME 1964;7: 834–43.
[36] Tozawa Y. Forming technology for raising the accuracy of sheet-formed products. Journal of Materials Processing Technology 1990;22:343–51.
[37] Zhang ZT, Lee D. Effect of process variables and material properties on the springback of 2d-draw bending parts. Automotive Stamping Technology 1995;11–8.
[38] Kuwabara T, Takahashi S, Ito K. Springback analysis of sheet metal subjected to bending–unbending under tension Part I (theory and results of numerical analysis). Advanced Technology of Plasticity. In: Altan T, editor. Proceedings of the 5th ICTP, vol. II. Columbus, Ohio, 1996. p. 743–6.
[39] Tang SC. Application of an anisotropic hardening rule to springback prediction. Advanced Technology of Plasticity. In: Altan T, editor. Proceedings of the 5th ICTP, vol. II. Columbus, Ohio, 1996. p. 719–22.
[40] Focellese A, Fratini L, Gabrielli F, Micari F. The evaluation of springback in 3d stamping and coining processes. Journal of Materials Processing Technology 1998;80–81:108–12.
[41] Kuwabara T, Seki N, Takahashi S. A rigorous numerical analysis of residual curvature of sheet metals subjected to bending–unbending under tension. In: Geiger M, editor. Advanced Technology of Plasticity 1999, vol. II. Berlin: Springer, 1999. p. 1071–5.
[42] Balakrishnan V. Measurement of in-plane Bauschinger effect in metal sheets. MS Thesis, The Ohio State University, 1999.
[43] Kuwabara T, Morita Y, Miyashita Y, Takahashi S. Elastic–plastic behavior of sheet metal subjected to in-plane reverse loading. Journal of Japanese Society of Technology and Plasticity 1995;36:769–74 (in Japanese).
[44] Jiang S. Springback investigations. MS Thesis. The Ohio State University, 1997.
[45] Shen Y. The reverse-bend test: indirect measurement of the bauschinger effect in metal sheets. MS Thesis. The Ohio State University, 1999.
[46] Zhang LC, Lu G, Leong S. V-shaped sheet forming by deformable punches. Journal of Materials Processing Technology 1997;63:134–9.
[47] Zhang LC, Lin Z. An analytical solution to springback of sheet metals stamped by a rigid punch and an elastic die. Journal of Materials Processing Technology 1997;63:49–54.
[48] Chou I, Hung C. Finite element analysis and optimization on springback reduction. International Journal of Machine Tools and Manufacture 1999;39:517–36.
[49] Hishida Y, Wagoner RH. Experimental analysis of blank holding force control in sheet forming, SAE Paper Number 930285, Sheet Metal and Stamping Symposium, SAE SP-944, Warrendale, PA, 1993. p. 93–100.
[50] Sunseri M, Karafillis AP, Cao J, Boyce MC. Methods to obtain net shape in aluminum sheet metal forming using active binder control. Mechanics in Materials Processing and Manufacturing (ASME) 1994;194:167–84.
[51] Sunseri M, Cao J, Karafillis AP, Boyce MC. Accommodation of springback error in channel forming using active binder force control: numerical simulations and experiments. Transactions of ASME 1996;118:426–35.
[52] Han SS, Park KC. An investigation of the factors influencing springback by empirical and simulative techniques. Proceedings of Numisheet'99, Besancon, France, 1999. p. 53–7.
[53] Nagai Y. High precision U-bending technique for moderately thick plate. Japanese Society of Technology and Plasticity 1987;28:143–9 (in Japanese).

[54] Kutt LM, Nardiello JA, Ogilvie PL, Pifko AB, Papazian JM. Non-linear finite element analysis of springback. Communications in Numerical Methods in Engineering 1999;15:33–42.
[55] United States Steel Corporation (US Steel) Material data sheet provided with the material, 1996.
[56] Aluminum Company of America (ALCOA) Material data sheet provided with the material, 1996.
[57] Annual Book of ASTM Standards, American Society of Testing and Materials, West Conshohocken, PA, vol. 3.01, Standard E-8M-96, 76-96.
[58] Hollomon JH. Tensile deformation. AIME Transactions 1945;162:268.
[59] Swift HW. Plastic instability under plane stress. Journal of Mechanics and Physics of Solids 1952;1:1.
[60] Voce E. The relationship between stress and strain for homogeneous deformation. Journal of the Institute of Metals 1948;74:537–62,760–71.
[61] Carden WD, Wagoner RH, Matlock DK. Unpublished research.
[62] Parco Prelube MP 404, manufactured and distributed by Parker Amchem, Henkel Surface Technologies Corporation, 32100 Stephenson Highway, Madison Heights Michigan, 48071, phone: (810) 583-9300.
[63] Wagoner RH, Carden WD, Carden WP, Matlock DK. Springback after drawing and bending of metal sheets. In: Chandra T, Leclair SR, Meech JA, Verma B, Smith M, Balachandran B, editors. Proceedings of the IPMM '97—Intelligent Processing and Manufacturing of Materials, University of Wollongong, 1997, vol. 1. p. 1–10.
[64] Li KP, Wagoner RH. In: Huetink J, Baaijens FPT, editors. Simulation of springback. Simulation of materials processing. Rotterdam: A.A. Balkema, 1998. p. 21–32.
[65] Li KP, Wagoner RH. Simulation of deep drawing with various elements. In: Gelin JC, Picart P, editors. Proceedings of NUMISHEET'99. University of Franche-Compte, Besancon, France, 1999. p. 151–6.
[66] Li KP, Geng LM, Wagoner RH. Simulation of springback with the draw/bend test. In: Meech JA, Veiga MM, Smith MH, LeClair SR, editors. IPMM'99, 1, IEEE. Vancouver, BC, Canada, ISBN 0-7803-5489-3.
[67] Li KP, Geng LM, Wagoner RH. Simulation of springback: choice of element. In: Geiger M, editor. Advanced technology of plasticity 1999, vol. III. Berlin: Springer, 1999. p. 2091–8.
[68] Geng LM, Wagoner RH. Springback analysis with a modified combined hardening law, sheet metal forming: Sing Tang 65th Anniversary Volume, SP-1536, SAE Publication 2000-01-0768. Warrendale, PA: Society of Automotive Engineers, 2000. p. 21–32.
[69] Wenner ML. Private communication, General Motors Corporation, March, 1996.
[70] Mickalich MK, Wenner ML. Calculation of springback and its variation in channel forming operations SAE Paper 880526, in P-206, Advances and Trends in Automotive Sheet Metal Stamping. Warrendale, PA: Society of Automotive Engineers, 1988. p. 99–100.
[71] Thompson NE, Ellen CH. A simple theory for "side-wall curl". Journal of Applied Metalworking 1985;4:1:39–42.
[72] Horrocks D, Johnson W. On anticlastic curvature with special reference to plastic bending: a literature survey and some experimental investigations. International Journal of Mechanical Sciences 1967;8:835–61.
[73] Young WC. Roark's formulas for stress and strain. 6th ed. Table I, Case 20. New York: McGraw-Hill, 1989. p. 68.